Anisotropic Thermal Properties of the Nonlinear Optical and Polar Oxide Material Na2TeW2O9

ARTICLE *in* CRYSTAL GROWTH & DESIGN · AUGUST 2011

Impact Factor: 4.89 · DOI: 10.1021/cg200659z

6 AUTHORS, INCLUDING:

Weiguo Zhang
University of Houston
26 PUBLICATIONS **356** CITATIONS
SEE PROFILE

Shiv Halasyamani
University of Houston
267 PUBLICATIONS **5,781** CITATIONS
SEE PROFILE

CRYSTAL GROWTH & DESIGN

ARTICLE

pubs.acs.org/crystal

Anisotropic Thermal Properties of the Nonlinear Optical and Polar Oxide Material $Na_2TeW_2O_9$

Weiguo Zhang and P. Shiv Halasyamani*

Department of Chemistry, University of Houston, 136 Fleming Building, Houston, Texas 77204-5003, United States

Zeliang Gao, Shanpeng Wang, Jian Wang, and Xutang Tao*

State Key Laboratory of Crystal Materials, Shandong University, Jinan 250100, P. R. China

ABSTRACT: Centimeter size crystals of the second-order nonlinear optical and polar oxide $Na_2TeW_2O_9$ (NTW) have been grown by the top-seeded solution growth method. The specific heat, anisotropic thermal expansion, and thermal diffusivity have been measured. In addition, the average principal thermal expansion coefficients have been calculated on the basis of measurements between 23 and 500 °C. NTW exhibits strongly anisotropic thermal expansion that can be attributed to its low symmetry, monoclinic, in space group *Ia*. The relationships between the structure and thermal properties are discussed.

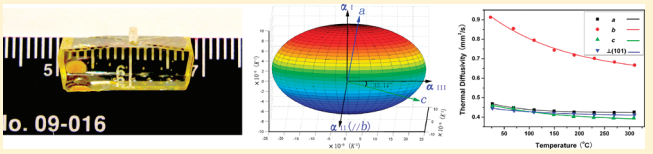

INTRODUCTION

Polar materials, i.e., those that exhibit a macroscopic dipole moment, have attracted much attention that can be attributed to their nonlinear optical, piezoelectric, pyroelectric, and ferroelectric properties and applications.[1−6] Inorganic materials are commonly used in these applications that can be attributed to their temperature stability, mechanical strength, and chemical inertness. To exhibit pyroelectric and ferroelectric properties, the material must be found in one of 10 polar crystal classes: 1, 2, 3, 4, 6, m, mm2, 3m, 4mm, and 6mm.[7,8] With oxides, new polar materials have been synthesized by using cations susceptible to second-order Jahn−Teller effects,[9−16] octahedrally coordinated d^0 transition metals and lone-pair cations.[17−49] With both families of cations, the local coordination environments are polar. When these local environments are aligned in the structure, a macroscopically polar material is observed. Some of the new polar materials exhibit very attractive functional properties, such as strong second-harmonic generation, based on powder measurements. Recently, two of these materials, $BaTeMo_2O_9$ (BTM)[39] and $Na_2TeW_2O_9$ (NTW),[36] have been grown as large, centimeter size, single crystals.[50,51] The detailed measurement of a host of physical properties, such as thermal expansion, thermal conductivity, and specific heat, may be performed on large single crystals. These measurements, on large single crystals of BTM, demonstrated the material to have piezoelectric and electro-optical applications, as well as applications for NLO behavior in the near- and mid-IR regions.[50,52,53] Additionally, the thermal properties of a material, such as the thermal expansion, thermal conductivity, and specific heat, will impact the potential applications. If a material exhibits large anisotropic thermal expansion, low specific heat, and low thermal conductivity, a large crystal of the material may be easily cracked during growth and processing if the temperature gradient is too large.[54,55]

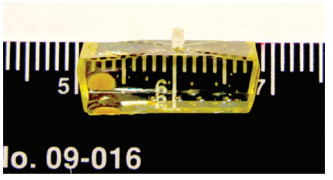

Figure 1. As-grown single crystal of $Na_2TeW_2O_9$. Note that the crystal exhibits high optical homogeneity. The spots are from the solid flux adhering to the single crystal.

To date, comprehensive thermal properties have only been measured and discussed on BTM single crystals.[56] In this paper, we report on the detailed thermal properties of NTW single crystals, including the thermal expansion, thermal conductivity, and specific heat. The relationships between structure and thermal properties of NTW are also discussed.

EXPERIMENTAL SECTION

Crystal Growth and Processing. As we reported previously,[51] NTW is an incongruently melting material. Centimeter size NTW single crystals were grown through the top-seeded solution growth (TSSG) method by using TeO_2 as flux, i.e., NTW:TeO_2 molar ratio of 1:0.4. By using the seed-testing method, the saturation temperature of the flux system was determined to be approximately 640 °C. Subsequently, a *c*-oriented seed was dipped into the flux and rotated at 20−40 rpm. The temperature was reduced at a rate of 0.5−1 °C/day as growth progressed. The time of growth ranged from 4 to 5 days. Figure 1 shows the as-grown NTW crystal with a size of 17 mm × 7 mm × 6 mm.

Received: May 24, 2011
Revised: June 9, 2011
Published: June 13, 2011

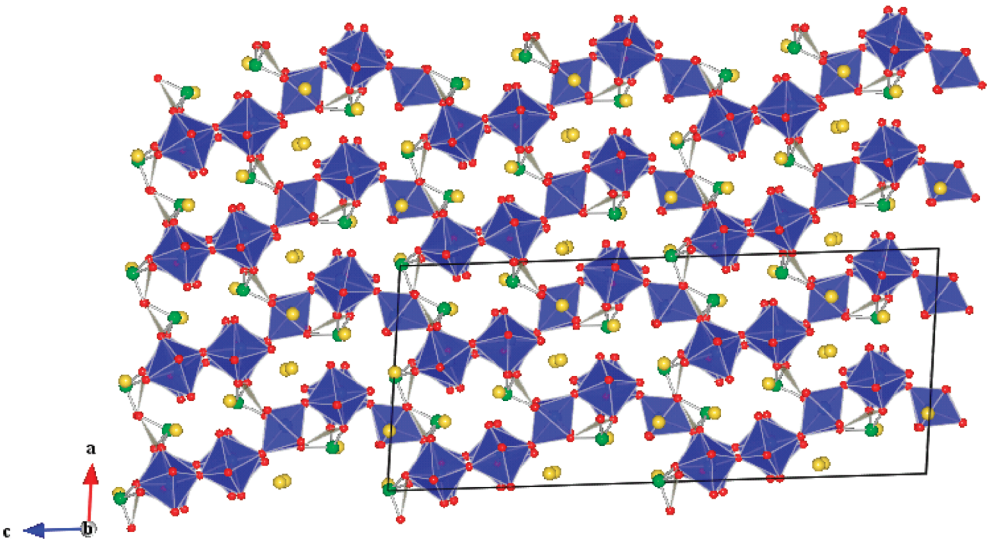

Figure 2. Polyhedral representation of the $Na_2TeW_2O_9$ crystal structure in the $a-c$ plane. The yellow, green, blue, and red spheres represent Na^+, Te^{4+}, W^{6+}, and O^{2-} ions, respectively. Note that along the a axis the WO_6 octahedra (blue polyhedra) are connected by TeO_3 groups, whereas along the c axis, a wavelike connectivity of the WO_6 octahedra is observed.

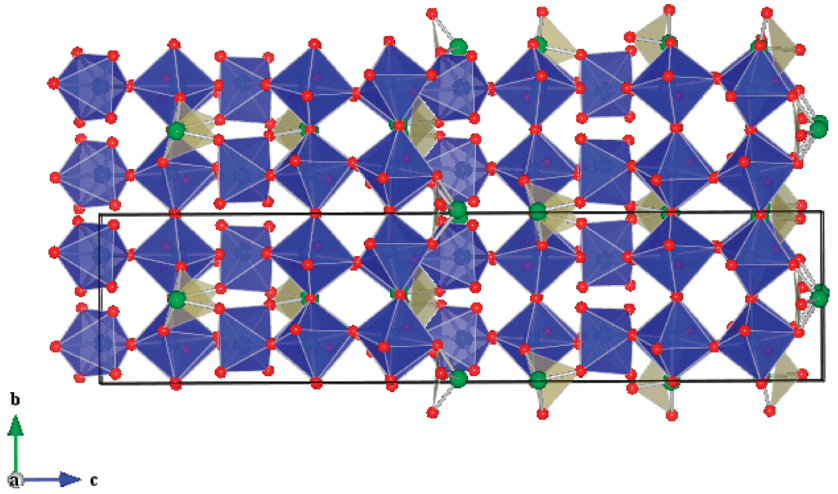

Figure 3. Polyhedral representation of the $Na_2TeW_2O_9$ crystal structure in the $b-c$ plane. The green, blue, and red spheres represent Te^{4+}, W^{6+}, and O^{2-} ions, respectively. Note that along the b axis there are six linear WO_6 octahedral chains (blue polyhedral) in one unit cell.

To measure the thermal properties, four different oriented wafers with a size of 4 mm × 4 mm × 1 mm were cut from this crystal.

Density Measurement. The density of NTW at room temperature (20 °C) was measured by the buoyancy method. Thirty milliliters of deionized water was added to an empty 50 mL beaker and weighed. A NTW crystal attached to a silver filament (Φ = 0.1 mm) was immersed in the water without touching the bottom of the beaker. The weight of the beaker and crystal was measured and the density determined. The entire process was repeated three times to obtain an average value.

Measurements of the Thermal Properties. The specific heat was measured by differential scanning calorimetry (Perkin-Elmer) using a simultaneous thermal analyzer (Diamond DSC) between 30 and 300 °C at a heating rate of 10 °C/min. The thermal expansion of the NTW crystal was measured up to 500 °C by using a thermal dilatometer (Diamond TMA). The four crystal wafers used for thermal expansion measurements were polished. Three pieces of wafers of the same size, 4 mm × 4 mm × 1 mm, having faces perpendicular to the a, b, and c crystallographic directions and the fourth one with a face parallel to the

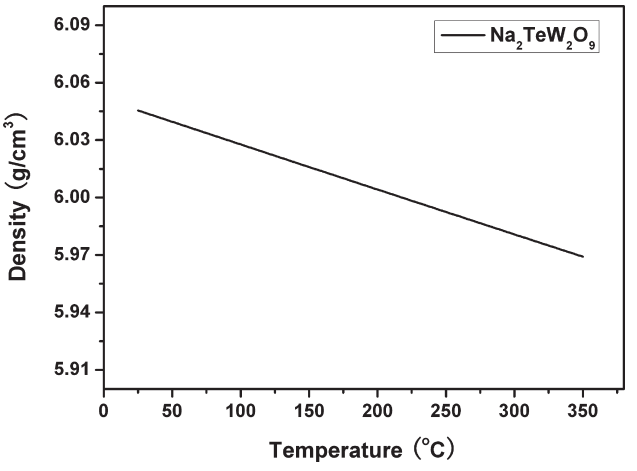

Figure 4. Calculated density vs temperature for a single crystal of $Na_2TeW_2O_9$.

dx.doi.org/10.1021/cg200659z |*Cryst. Growth Des.* 2011, 11, 3636–3641

(101) plane were coated with graphite on both sides and were used to take the measurements. The thermal diffusivity coefficient was measured by the laser flash method using a laser flash apparatus (NETZSCH LFA 447 Nanoflash) from 24 to 300 °C.

RESULTS AND DISCUSSION

Structure. As the atomic positions, bond lengths, and bond angles of NTW have been discussed in detail,[36] we will focus on the connectivity of the WO_6 octahedra. Polyhedral representations of NTW in the $a-c$ and $b-c$ planes are shown in Figures 2 and 3, respectively.[57] As seen in Figure 2, "wavelike" connectivity of the WO_6 octahedra is observed along the c axis, whereas linear chains of WO_6 octahedra are observed along the b axis (see Figure 3). Interestingly, along the a axis, the WO_6 octahedra are not directly connected but are linked through TeO_3 polyhedra.

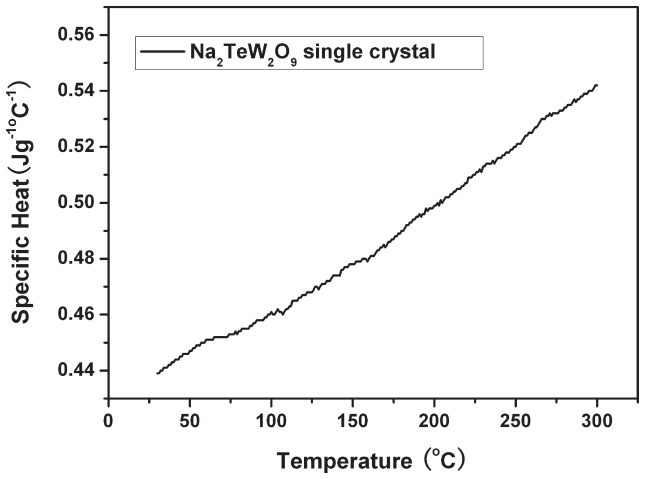

Figure 5. Specific heat vs temperature for a single crystal of $Na_2TeW_2O_9$.

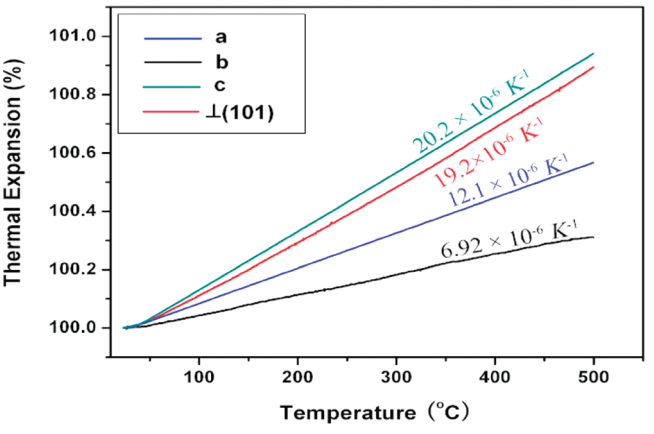

Figure 6. Thermal expansion along different crystallographic directions of a single crystal of $Na_2TeW_2O_9$.

As we will show, this difference in connectivity along the a, b, and c axes directly impacts the observed thermal properties.

Density. The average density, determined by the buoyancy method, of a NTW single crystal at 20 °C is 6.07(6) g/cm^3, which is in good agreement with the calculated value of 6.045(5) g/cm^3 from the crystal structure. The density values at different temperatures, calculated through the thermal expansion coefficients, are shown in Figure 4. From Figure 4, we can see that the density of the NTW crystal decreases linearly with an increasing temperature.

Specific Heat. For nonlinear optical crystals, the damage threshold and therefore its possible applications can be greatly influenced by the specific heat.[55] The specific heat of the NTW crystal varying as a function of temperature is shown in Figure 5. The specific heat increases almost linearly from 0.43(9) to 0.54(2) J g^{-1} K^{-1} as the temperature is increased from 30 to 300 °C, indicating that NTW crystals can tolerate more thermal energy at high temperatures.

Thermal Expansion. The thermal expansion coefficient, α, is a second-rank symmetric tensor. The maximum number of independent constants is six, but this number can be reduced for higher-symmetry crystals.[58] For the monoclinic NTW crystal, the thermal expansion coefficient tensor with respect to the crystallographic axes in the conventional orientation is

$$\begin{bmatrix} \alpha_{11} & 0 & \alpha_{13} \\ 0 & \alpha_{22} & 0 \\ \alpha_{31} & 0 & \alpha_{33} \end{bmatrix} \quad (1)$$

There are four independent principal thermal components, α_{11}, α_{31} ($=\alpha_{13}$), α_{22}, and α_{33}. To determine α_{ij}, we cut samples from the crystal along four different orientations. In the (010) plane, the expansion coefficients corresponding to the three

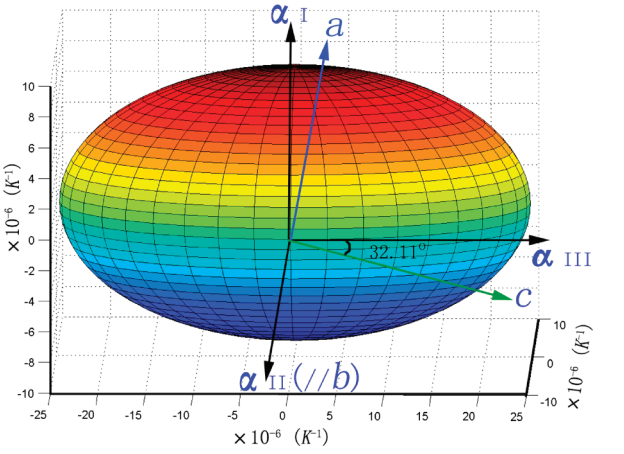

Figure 7. Thermal expansion ellipsoid for a single crystal of $Na_2TeW_2O_9$. Notice the crystallographic coordinates have a clockwise rotation along the b axis to yield the conventional coordinates.

Table 1. Measured and Calculated Thermal Expansion Coefficients of a $Na_2TeW_2O_9$ Single Crystal

NTW thermal expansion coefficient ($\times 10^{-6}$ K^{-1})										
measured				calculated						
α_a	α_b	α_c	$\alpha_{\perp(101)}$	α_{11}	α_{22}	α_{33}	α_{31}	α_{I}	α_{II}	α_{III}
12.1(1)	6.9(2)	20.2(1)	19.2(2)	13.2(9)	6.9(2)	20.2(1)	7.1(5)	8.8(1)	6.9(2)	24.6(9)

dx.doi.org/10.1021/cg200659z |Cryst. Growth Des. 2011, 11, 3636–3641

Table 2. Measured (top) and Calculated (bottom) Thermal Expansion Coefficients of $Na_2TeW_2O_9$ and $BaTeMo_2O_9$ Crystals along Different Directions

measured thermal expansion coefficient ($\times 10^{-6}$ K^{-1})							
$Na_2TeW_2O_9$				$BaTeMo_2O_9$[a]			
α_a	α_b	α_c	$\alpha_{\perp(101)}$	α_a	α_b	α_{a^*}	α_{c^*}
12.1(1)	6.9(2)	20.2(1)	19.2(2)	16.7(1)	9.2(3)	16.8(4)	13.0(5)

	calculated principal thermal expansion coefficient ($\times 10^{-6}$ K^{-1})		
	α_I	α_{II}	α_{III}
$Na_2TeW_2O_9$	8.8(1)	6.9(2)	24.6(9)
$BaTeMo_2O_9$[a]	10.4(6)	9.2(3)	19.3(1)

[a] From ref 56.

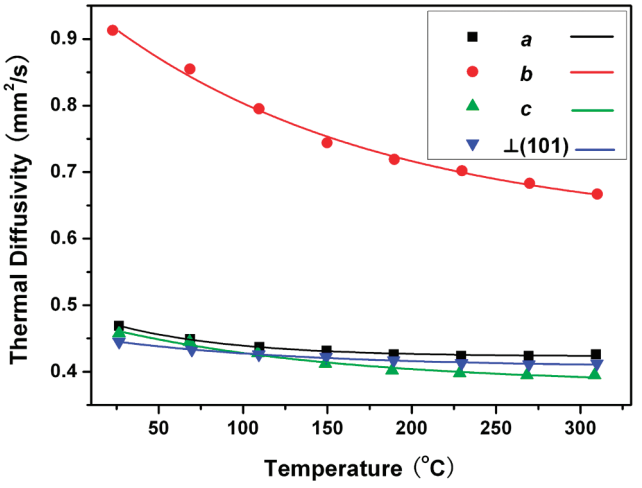

Figure 8. Thermal diffusivity coefficients, experimental (symbols) and nonlinear fits (solid lines), along different directions of a single crystal of $Na_2TeW_2O_9$.

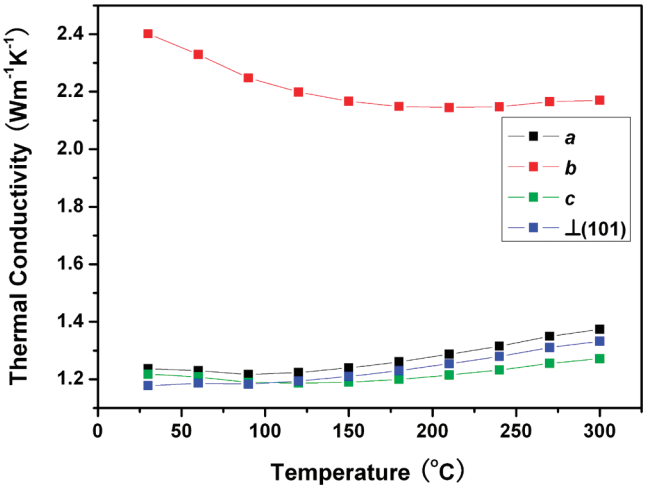

Figure 9. Calculated thermal conductivity of a single crystal of $Na_2TeW_2O_9$ along different crystallographic directions.

orientations ($\xi_1 = 0 \pm 0.05°$, $\xi_2 = 68.12 \pm 0.05°$, and $\xi_3 = 95.02 \pm 0.05°$) measured with respect to the crystallographic c axis are along the c axis, perpendicular to the (101) plane, and along the a vector, respectively. The solid lines in Figure 6 are the thermal expansion ratio curves along the crystallographic axes. It can be seen that the expansion ratio is almost linear over the entire measured temperature range, and NTW exhibits expansion when heated. Thus, all the thermal expansion coefficients are positive along different crystallographic directions. The average linear thermal expansion coefficient for the crystallographic directions can be calculated with the following formula:

$$\overline{\alpha}(T_0 \rightarrow T) = \frac{\Delta L}{L_0}\frac{1}{\Delta T} \qquad (2)$$

where $(T_0 \rightarrow T)$ is the average linear thermal expansion coefficient over the temperature range from T_0 to T, L_0 is the sample length at T_0, ΔL is the length change when the temperature changes from T_0 to T, and temperature change $\Delta T = T - T_0$.

The average values of the linear thermal expansion coefficients of the NTW crystal from 20 to 500 °C are as follows: $\alpha_c = 20.2(1) \times 10^{-6}$ K^{-1}, $\alpha_{\perp(101)} = 19.2(2) \times 10^{-6}$ K^{-1}, $\alpha_a = 12.1(1) \times 10^{-6}$ K^{-1}, and $\alpha_b = 6.9(2) \times 10^{-6}$ K^{-1}. By using the related equations presented in refs 58 and 59, the three coefficients α_{11}, α_{31}, and α_{33} were calculated to be $13.2(9) \times 10^{-6}$, $7.1(5) \times 10^{-6}$, and $20.2(1) \times 10^{-6}$ K^{-1}, respectively. In addition, the expansion coefficient α_{22} in the direction of the crystallographic b axis has been calculated to be $6.9(2) \times 10^{-6}$ K^{-1}, the same value as α_b. Thus, for the monoclinic NTW crystal, the principal thermal expansion coefficients α_I, α_{II}, and α_{III} are calculated to be $8.8(1) \times 10^{-6}$, $6.9(2) \times 10^{-6}$, and $24.6(9) \times 10^{-6}$ K^{-1}, respectively. The orientation of the principal axis φ is calculated to be 32.11°, where φ is the angle measured clockwise from the α_{III} axis toward the crystallographic c axis (the α_{II} axis coincides with the b axis). The measured and calculated values along different axes are listed in Table 1. The relationship between crystallographic orientation and conventional orientation is shown in Figure 7.

For the crystallographic axes, the thermal expansion coefficients are as follows: $\alpha_a = 12.1(1) \times 10^{-6}$ K^{-1}, $\alpha_b = 6.9(2) \times 10^{-6}$ K^{-1}, and $\alpha_c = 20.2(1) \times 10^{-6}$ K^{-1}. The relatively large difference between these values can be understood by examining the NTW crystal structure. It is suggested that larger thermal coefficient values will be observed when the structure has the most flexibility. As seen in Figure 2, this is clearly along the a and c axes. More rigid connectivity is observed along the b

dx.doi.org/10.1021/cg200659z |Cryst. Growth Des. 2011, 11, 3636–3641

axis (see Figure 3); thus, the thermal expansion coefficient is the smallest in that direction.

Compared with those of BTM, the thermal expansion coefficients of NTW are different, even though both materials are in the same monoclinic crystal class and have similar stoichiometries and polyhedral building blocks. The thermal expansion coefficients of both crystals are listed in Table 2. From Table 2, it is clear that NTW exhibits stronger anisotropic thermal expansion than BTM. We suggest this is mainly attributable to the different polyhedral connectivities in both materials. The large anisotropic thermal expansion of the NTW crystal suggests more caution should be taken to protect the crystal from cracking caused by thermal expansion during crystal growth, processing, and applications.

Thermal Diffusivity and Thermal Conductivity. The thermal diffusivity coefficients of NTW were measured directly along the *a*, *b*, and *c* axes and perpendicular to the (101) plane (see Figure 8). As seen in Figure 8, it is clear that the thermal diffusivity coefficients decrease with an increase in temperature. At higher temperatures, the thermal diffusivity coefficients are almost constant. Also, the thermal diffusivity coefficient along the *b* axis is much larger than those along the other three directions, consistent with the strong anisotropy of the NTW structure. Interestingly, the thermal diffusivity coefficients along the *a* and *c* axes and perpendicular to the (101) plane are very close to each other, which indicates weak anisotropy in the (010) plane. Additionally, the thermal conductivity *k* can be calculated by using the following equation:

$$\kappa = \lambda \rho C_p \qquad (3)$$

where κ, λ, ρ, and C_p denote the principal thermal conductivity, the thermal diffusivity coefficient, the density, and the specific heat of the crystal, respectively. As the density and specific heat are scalars, the thermal conductivities along the different directions are mainly influenced by thermal diffusivities. Thus, the thermal conductivities along the different directions were calculated according to eq 3, and the data are shown in Figure 9. From Figure 9, we can see that the thermal conductivities of NTW single crystals exhibit different trends along different directions as the temperature changes. Along *b* axis, the thermal conductivity decreases with an increase in temperature. However, along the other three directions, the thermal conductivities are almost constant when the temperature is below 100 °C, and above this temperature, the thermal conductivities become larger as the temperature increases, indicating NTW crystals can tolerate more thermal load at high temperatures. This phenomenon is also observed for monoclinic crystals such as BTM[56] and $KYb(WO_4)_2$.[60]

CONCLUSION

The anisotropic thermal properties of a single crystal of NTW were carefully studied by measuring the thermal expansion, specific heat, and thermal diffusivity and calculating the thermal conductivity. The measured (calculated) values of the thermal expansion coefficients are 12.1×10^{-6} K^{-1} [$8.8(1) \times 10^{-6}$ K^{-1}], $6.9(2) \times 10^{-6}$ K^{-1} [$6.9(2) \times 10^{-6}$ K^{-1}], and $20.2(1) \times 10^{-6}$ K^{-1} [$24.6(9) \times 10^{-6}$ K^{-1}] for α_a (α_I), α_b (α_{II}), and α_c (α_{III}), respectively. We have determined that single crystals of NTW exhibit relatively large anisotropic thermal expansion, indicating that care should be taken during crystal growth and processing. We are in the process of growing large single crystals of other functional materials and will be reporting on them in the near future.

AUTHOR INFORMATION

Corresponding Author

*E-mail: psh@uh.edu or txt@icm.sdu.edu.cn.

ACKNOWLEDGMENT

W.Z. and P.S.H. thank the Robert A. Welch Foundation (Grant E-1457), the Texas Center for Superconductivity, and the National Science Foundation (DMR-0652150) for support. Z.G., S.W., J.W., and X.T. thank the National Natural Science Foundation of China (Grants 51021062 and 50990061) and the 973 Program of the People's Republic of China (Grant 2010CB630702) for financial support of this work.

REFERENCES

(1) Nye, J. F. *Physical Properties of Crystals*; Oxford University Press: Oxford, U.K., 1957.
(2) Cady, W. G. *Piezoelectricity: An Introduction to the Theory and Applications of Electromechanical Phenomena in Crystals*; Dover: New York, 1964.
(3) Lang, S. B. *Sourcebook of Pyroelectricity*; Gordon & Breach Science: London, 1974.
(4) Jona, F.; Shirane, G. *Ferroelectric Crystals*; Pergamon Press: Oxford, U.K., 1962.
(5) Waser, R.; Böttger, U.; Tiedke, S. *Polar Oxides: Properties, Characterization, and Imaging*; Wiley-VCH Verlag GmbH & Co. KGaA: Weinheim, Germany, 2005.
(6) Marder, S. R.; Sohn, J. E.; Stucky, G. D. *Materials for Non-Linear Optics: Chemical Perspectives*; American Chemical Society: Washington, DC, 1991.
(7) Hahn, T. *International Tables for Crystallography, Vol. A, Space Group Symmetry*; Kluwer Academic: Dordrecht, The Netherlands, 2006.
(8) Halasyamani, P. S.; Poeppelmeier, K. R. *Chem. Mater.* **1998**, *10*, 2753.
(9) Opik, U.; Pryce, M. H. L. *Proc. R. Soc. London, Ser. A* **1957**, *238*, 425.
(10) Bader, R. F. W. *Mol. Phys.* **1960**, *3*, 137.
(11) Bader, R. F. W. *Can. J. Chem.* **1962**, *40*, 1164.
(12) Pearson, R. G. *J. Am. Chem. Soc.* **1969**, *91*, 4947.
(13) Pearson, R. G. *THEOCHEM* **1983**, *103*, 25.
(14) Wheeler, R. A.; Whangbo, M. H.; Hughbanks, T.; Hoffmann, R.; Burdett, J. K.; Albright, T. A. *J. Am. Chem. Soc.* **1986**, *108*, 2222.
(15) Kunz, M.; Brown, I. D. *J. Solid State Chem.* **1995**, *115*, 395.
(16) Goodenough, J. B. *Annu. Rev. Mater. Sci.* **1998**, *28*, 1.
(17) Heier, K. R.; Norquist, A. J.; Halasyamani, P. S.; Duarte, A.; Stern, C. L.; Poeppelmeier, K. R. *Inorg. Chem.* **1999**, *38*, 762.
(18) Welk, M. E.; Norquist, A. J.; Stern, C. L.; Poeppelmeier, K. R. *Inorg. Chem.* **2000**, *39*, 3946.
(19) Welk, M. E.; Norquist, A. J.; Stern, C. L.; Poeppelmeier, K. R. *Inorg. Chem.* **2001**, *40*, 5479.
(20) Welk, M. E.; Norquist, A. J.; Arnold, F. P.; Stern, C. L.; Poeppelmeier, K. R. *Inorg. Chem.* **2002**, *41*, 5119.
(21) Izumi, H. K.; Kirsch, J. E.; Stern, C. L.; Poeppelmeier, K. R. *Inorg. Chem.* **2005**, *44*, 884.
(22) Marvel, M. R.; Lesage, J.; Baek, J.; Halasyamani, P. S.; Stern, C. L.; Poeppelmeier, K. R. *J. Am. Chem. Soc.* **2007**, *129*, 13963.
(23) Welk, M. E.; Stern, C. L.; Poeppelmeier, K. R.; Norquist, A. J. *Cryst. Growth Des.* **2007**, *7*, 956.
(24) Smit, J. P.; McDonald, T. M.; Poeppelmeier, K. R. *Solid State Sci.* **2008**, *10*, 396.
(25) Marvel, M. R.; Pinlac, R. A. F.; Lesage, J.; Stern, C. L.; Poeppelmeier, K. R. *Z. Anorg. Allg. Chem.* **2009**, *635*, 869.

(26) Chamberlain, J. M.; Albrecht, T. A.; Lesage, J.; Sauvage, F.; Stern, C. L.; Poeppelmeier, K. R. *Cryst. Growth Des.* **2010**, *10*, 4868.
(27) Enterkin, J. A.; Maggard, P. A.; Ishiwata, S.; Marks, L. D.; Poeppelmeier, K. R.; Azuma, M.; Takano, M. *J. Solid State Chem.* **2010**, *183*, 551.
(28) Sauvage, F.; Bodenez, V.; Tarascon, J.-M.; Poeppelmeier, K. R. *J. Am. Chem. Soc.* **2010**, *132*, 6778.
(29) Kong, F.; Huang, S.-P.; Sun, Z.-M.; Mao, J.-G.; Cheng, W.-D. *J. Am. Chem. Soc.* **2006**, *128*, 7750.
(30) Jiang, H.-L.; Huang, S.-P.; Fan, Y.; Mao, J.-G.; Cheng, W.-D. *Chem.—Eur. J.* **2008**, *14*, 1972.
(31) Hu, T.; Qin, L.; Kong, F.; Zhou, Y.; Mao, J.-G. *Inorg. Chem.* **2009**, *48*, 2193.
(32) Sun, C.-F.; Hu, C.-L.; Xu, X.; Ling, J.-B.; Hu, T.; Kong, F.; Long, X. F.; Mao, J.-G. *J. Am. Chem. Soc.* **2009**, *131*, 9486.
(33) Balraj, V.; Vidyasagar, K. *Inorg. Chem.* **1998**, *37*, 4764.
(34) Porter, Y.; Ok, K. M.; Bhuvanesh, N. S. P.; Halasyamani, P. S. *Chem. Mater.* **2001**, *13*, 1910.
(35) Welk, M. E.; Norquist, A. J.; Arnold, F. P.; Stern, C. L.; Poeppelmeier, K. R. *Inorg. Chem.* **2002**, *41*, 5119.
(36) Goodey, J.; Broussard, J.; Halasyamani, P. S. *Chem. Mater.* **2002**, *14*, 3174.
(37) Porter, Y.; Halasyamani, P. S. *J. Solid State Chem.* **2003**, *174*, 441.
(38) Goodey, J.; Ok, K. M.; Broussard, J.; Hofmann, C.; Escobedo, F. V.; Halasyamani, P. S. *J. Solid State Chem.* **2003**, *175*, 3.
(39) Ra, H.-S.; Ok, K. M.; Halasyamani, P. S. *J. Am. Chem. Soc.* **2003**, *125*, 7764.
(40) Hou, J. Y.; Huang, C. C.; Zhang, H. H.; Tu, C. Y.; Sun, R. Q.; Yang, Q. Y. *J. Mol. Struct.* **2006**, *785*, 37.
(41) Chi, E. O.; Ok, K. M.; Porter, Y.; Halasyamani, P. S. *Chem. Mater.* **2006**, *18*, 2070.
(42) Sivakumar, T.; Ok, K. M.; Halasyamani, P. S. *Inorg. Chem.* **2006**, *45*, 3602.
(43) Kim, J.-H.; Baek, J.; Halasyamani, P. S. *Chem. Mater.* **2007**, *19*, 5637.
(44) Chang, H. Y.; Sivakumar, T.; Ok, K. M.; Halasyamani, P. S. *Inorg. Chem.* **2008**, *47*, 8511.
(45) Chang, H. Y.; Kim, S. H.; Halasyamani, P. S.; Ok, K. M. *J. Am. Chem. Soc.* **2009**, *131*, 2426.
(46) Chang, H. Y.; Kim, S. H.; Ok, K. M.; Halasyamani, P. S. *J. Am. Chem. Soc.* **2009**, *131*, 6865.
(47) Chang, H. Y.; Kim, S. H.; Ok, K. M.; Halasyamani, P. S. *Chem. Mater.* **2009**, *21*, 1654.
(48) Kim, S. H.; Yeon, J.; Halasyamani, P. S. *Chem. Mater.* **2009**, *21*, 5335.
(49) Chang, H. Y.; Kim, S. W.; Halasyamani, P. S. *Chem. Mater.* **2010**, *22*, 3241.
(50) Zhang, W. G.; Tao, X. T.; Zhang, C. Q.; Gao, Z. L.; Zhang, Y. Z.; Yu, W. T.; Cheng, X. F.; Liu, X. S.; Jiang, M. H. *Cryst. Growth Des.* **2008**, *8*, 304.
(51) Zhang, W.; Li, F.; Kim, S. H.; Halasyamani, P. S. *Cryst. Growth Des.* **2010**, *10*, 4091.
(52) Gao, Z.; Tao, X.; Yin, X.; Zhang, W.; Jiang, M. *Appl. Phys. Lett.* **2008**, *93*, 252906.
(53) Gao, Z.; Yin, X.; Zhang, W.; Wang, S.; Jiang, M.; Tao, X. *Appl. Phys. Lett.* **2009**, *95*, 151107.
(54) Hou, W. B.; Xu, D.; Yuan, D. R.; Liu, M. G.; Zhang, N.; Tao, X. T.; Sun, S. Y.; Jiang, M. H. *Cryst. Res. Technol.* **1994**, *29*, 939.
(55) Xu, D.; Zhang, K. C.; Zhang, L. H. *Science and Technology of Crystal Growth Science*; Beijing, 1997 (in Chinese).
(56) Zhang, W.; Tao, X.; Zhang, C.; Zhang, H.; Jiang, M. *Cryst. Growth Des.* **2009**, *9*, 2633.
(57) Momma, K.; Izumi, F. *J. Appl. Crystallogr.* **2008**, *41*, 653.
(58) Krishnan, R. S.; Srinivasan, R.; Devanarayanan, S. *Thermal Expansion of Crystals*; Pergamon: Oxford, U.K., 1979.
(59) Liu, X. J.; Wang, Z. Y.; Wang, X. Q.; Zhang, G. H.; Xu, S. X.; Duan, A. D.; Zhang, S. J.; Sun, Z. H.; Xu, D. *Cryst. Growth Des.* **2008**, *8*, 2270.
(60) Zhao, H. Y.; Wang, J. Y.; Li, J.; Xu, G. G.; Zhang, H. J.; Yu, L. L.; Gao, W. L.; Xia, H. R.; Boughton, I. R. *Cryst. Growth Des.* **2008**, *8*, 3978.